

# Precision Mass Measurements beyond $^{132}\text{Sn}$ : Anomalous behaviour of odd-even staggering of binding energies

J. Hakala,\* J. Dobaczewski, D. Gorelov, T. Eronen,† A. Jokinen, A. Kankainen, V.S. Kolhinen, M. Kortelainen, I. D. Moore, H. Penttilä, S. Rinta-Antila, J. Rissanen, A. Saastamoinen, V. Sonnenschein, and J. Äystö‡  
 Department of Physics, P.O. Box 35 (YFL), FI-40014 University of Jyväskylä, Finland

(Dated: December 2, 2024)

Atomic masses of the neutron-rich isotopes  $^{121-128}\text{Cd}$ ,  $^{129,131}\text{In}$ ,  $^{130-135}\text{Sn}$ ,  $^{131-136}\text{Sb}$ , and  $^{132-140}\text{Te}$  have been measured with high precision (10 ppb) using the Penning trap mass spectrometer JYFLTRAP. Among these, the masses of four r-process nuclei  $^{135}\text{Sn}$ ,  $^{136}\text{Sb}$ , and  $^{139,140}\text{Te}$  were measured for the first time. The data reveals a strong  $N=82$  shell gap at  $Z=50$  but indicates the importance of correlations for  $Z > 50$ . An empirical neutron pairing gap expressed as the odd-even staggering of isotopic masses shows a strong quenching across  $N=82$  for Sn, with the  $Z$ -dependence that is unexplainable by the current theoretical models.

PACS numbers: 21.10.Dr, 21.60.-n, 27.60.+j

The doubly magic  $^{132}\text{Sn}$  nucleus has been probed intensively by nuclear spectroscopy over the last two decades. It has been found to exhibit features of exceptional purity for its single particle structure [1, 2]. This provides an ideal starting point for exploring detailed evolution of nuclear structure of more neutron-rich nuclei beyond the  $N=82$  closed shell in the vicinity of Sn. Only a few experimental and theoretical attempts along these lines have been performed recently. No experimental data exist for excited states or masses for nuclides below Sn with  $N > 82$ . The experimental situation is slightly better for  $Z > 50$  isotopes of Sb and Te because of their easier access.

Recent data on the  $B(E2)$  transition strengths for  $^{132}\text{Te}$ ,  $^{134}\text{Te}$  and  $^{136}\text{Te}$  isotopes [3] and their interpretation using a quadrupole-plus-pairing Hamiltonian and QRPA [4] suggested the need for reduced neutron pairing to explain the observed anomalous asymmetry in the  $B(E2)$  values across the  $N=82$  neutron shell. This behaviour was not observed in standard shell model calculations [3]. Another shell model calculation of the binding energies of heavy Sn isotopes with  $A > 133$  [5] suggested the importance of pairing correlations and the strength of the pairing interaction in general for weakly bound nuclei. Therefore, it would be necessary to probe the evolution of odd-even staggering of masses [6] around the  $N=82$  neutron shell to learn about the magnitude of pairing and its variation as a function of  $Z$  and  $N$  beyond  $^{132}\text{Sn}$ .

High precision of present-day ion-trap mass spectrometry combined with high sensitivity can provide the needed information on mass differences such as one- and two-nucleon separation energies, shell gaps and empirical pairing energies. For example, the masses of neutron-rich Sn and Xe isotopes were recently measured up to  $^{134}\text{Sn}$  and  $^{146}\text{Xe}$  respectively, with ISOLTRAP [7, 8]. In this Letter we wish to present new data of high-precision mass measurements of neutron-rich Cd, In, Sn, Sb, and Te isotopes across the  $N=82$  neutron shell by using the JYFLTRAP Penning trap. These nuclides are also of interest for nuclear astrophysics models of element synthesis, in particular, to

explain the large r-process abundance peak at  $A=130$  [9], see Fig. 1.

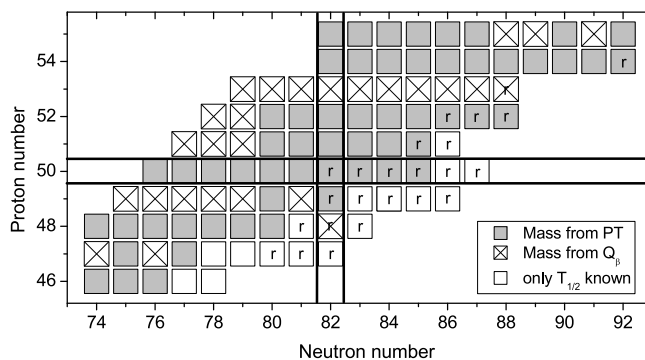


FIG. 1. Neutron-rich isotopes whose masses have been measured with a Penning trap (PT). Letter  $r$  denotes r-process nuclei according to Ref. [9].

The measurements were performed using the JYFLTRAP Penning trap mass spectrometer [10] which is connected to the Ion Guide Isotope Separator On-Line (IGISOL) mass separator [11]. The ions of interest were produced in proton-induced fission reactions by bombarding a natural uranium target with a proton beam of 25 MeV energy. A thorium target was used in the case of  $^{129}\text{In}$  and isotopes of Sb.

The fission products were stopped in a helium-filled gas cell at a pressure of about 200 mbar as singly-charged ions. The ions were transported out of the gas cell by helium flow and guided through a sextupole ion-guide before acceleration to 30 keV energy. A  $55^\circ$  bending magnet and a slit allowed only the ions with the selected mass number to pass towards a gas-filled radio frequency quadrupole cooler and buncher. After the cooler, the ions were guided to the Penning trap setup.

JYFLTRAP consists of two cylindrical Penning traps, the purification and precision trap, which are located inside a 7-T superconducting magnet. In Penning trap an ion has

three different eigenmotions: axial motion ( $\nu_z$ ) and two radial motions, magnetron ( $\nu_-$ ) and modified cyclotron ( $\nu_+$ ) motion. The frequencies of the radial motions sum in first order to the cyclotron frequency  $\nu_c = \frac{1}{2\pi} \frac{q}{m} B$ . Here  $q$  and  $m$  are the charge and mass of the ion, and  $B$  is the magnetic field.

Both traps were used to purify the samples, first with the sideband cooling technique [12] and then, if required, with the so-called Ramsey cleaning technique [13]. After a cleaned sample was trapped in the precision trap, the time-of-flight ion-cyclotron resonance (TOF-ICR) technique [14] was applied in order to determine the resonance frequency. The Ramsey method of separated oscillatory fields [15], which makes the sidebands more pronounced and narrower, was used in the majority of measurements. The experimental setup and the measurement technique are described in more detail in Ref. [16].

A sample resonance is shown in Fig. 2. When the cyclotron frequencies of an unknown species ( $m_{\text{meas}}$ ) and a well-known reference ion ( $m_{\text{ref}}$ ) are known, and both are singly charged ions, the atomic mass can be determined:

$$m_{\text{meas}} = \frac{\nu_{c,\text{ref}}}{\nu_{c,\text{meas}}} (m_{\text{ref}} - m_e) + m_e, \quad (1)$$

where  $m_e$  is the mass of the electron. The data analysis procedure was almost identical compared to [16]. In this work, the systematic uncertainties due to the magnetic field fluctuations were minimised by applying so-called interleaved frequency scanning described in Ref. [17].

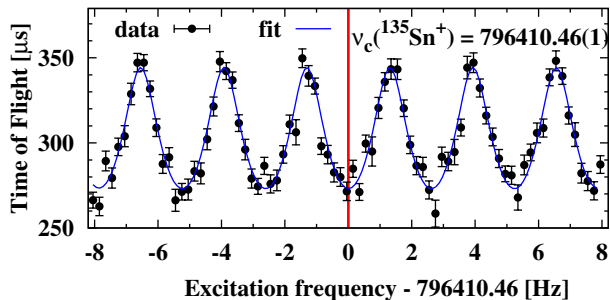


FIG. 2. (Color online) A time-of-flight (TOF) resonance from the JYFLTRAP setup for  $^{135}\text{Sn}^+$ . A two-fringe Ramsey pattern of 25-350-25 ms (*on-off-on*) was used in this case.

The results are given in Table I. Excitation times between 100 ms and 800 ms were used depending on the half-life of the isotope. In the case of Ramsey excitations, excitation patterns with two 25 ms pulses separated by a waiting time, were used. Table I lists only the masses of the ground states which are relevant for the further discussion of the results. A paper containing the isomeric data will be submitted separately. The new data agrees with the earlier ion-trap measurements and presents significant improvement in accuracy for all Sn, Sb and Te isotopes beyond  $N=82$ . This enables a critical evaluation of odd-even effects related to neutron pairing in these nuclides.

TABLE I. Cyclotron frequency ratios  $\bar{r}$  and resulting ground state mass excess values in keV based on this work. Masses of reference Xe isotopes for given  $A$  (ref.) are from [18–20]. The newest previous experimental data are given in the last column. Results from direct mass measurements are from ISOLTRAP [7, 21, 22] and FRS-ESR [23]. Otherwise, the value from AME2003 [18] is given.

ref.	nuclide	$\bar{r} = \frac{\nu_{c,\text{ref}}}{\nu_{c,\text{meas}}}$	JYFLTRAP	other	ref.
130	$^{121}\text{Cd}^\dagger$	0.930790292(23)	-81074.2(28)	-81060(80)	[18]
	$^{122}\text{Cd}$	0.938492175(22)	-80610.8(27)	-80616.6(44)	[22]
	$^{123}\text{Cd}^\dagger$	0.946216645(22)	-77414.4(26)	-77367(93)	[22]
	$^{124}\text{Cd}$	0.953920584(26)	-76702(4)	-76697(10)	[22]
	$^{125}\text{Cd}^\dagger$	0.961646357(24)	-73348.1(29)	-73360(70)	[18]
	$^{126}\text{Cd}$	0.969353430(25)	-72257(3)	-72256.5(42)	[22]
	$^{127}\text{Cd}$	0.97708259(18)	-68493(21)	-68520(70)	[18]
	$^{128}\text{Cd}$	0.984791049(83)	-67234(10)	-67250(17)	[22]
	$^{129}\text{In}^\dagger$	0.992442788(22)	-72838.0(26)	-72940(40)	[18]
	$^{131}\text{In}^\dagger$	1.007878672(22)	-68025.0(26)	-68137(28)	[18]
	$^{130}\text{Sn}^\dagger$	1.00080552(28)	-80133(4)	-80134(16)	[21]
132	$^{131}\text{Sn}$	0.992516774(26)	-77263(20) <sup>x</sup>	-77264(10)	[7]
	$^{132}\text{Sn}$	1.000103654(26)	-76543(4)	-76547(7)	[7]
134	$^{133}\text{Sn}$	0.992670308(18)	-70874.4(24)	-70847(23)	[7]
	$^{134}\text{Sn}$	1.000173910(25)	-66432(4)	-66320(150)	[7]
130	$^{135}\text{Sn}$	1.038731983(25)	-60632(3)		
	$^{131}\text{Sb}$	1.007763324(18)	-81982.5(21)	-81988(21)	[18]
	$^{132}\text{Sb}^\dagger$	1.015480774(22)	-79635.6(27)	-79674(14)	[18]
	$^{133}\text{Sb}$	1.023184733(31)	-78921(4)	-78943(25)	[18]
	$^{134}\text{Sb}^\dagger$	1.030923280(17)	-74021.1(21)	-74170(40)	[18]
	$^{135}\text{Sb}$	1.038657131(24)	-69689.6(29)	-69710(100)	[18]
	$^{136}\text{Sb}$	1.046397992(52)	-64510(7)		
	$^{132}\text{Te}$	1.015434872(33)	-85190(4)	-85182(7)	[18]
	$^{133}\text{Te}^\dagger$	1.023151534(18)	-82938.2(22)	-82945(24)	[18]
	$^{134}\text{Te}$	1.030852922(27)	-82535(4)	-82559(11)	[18]
	$^{135}\text{Te}$	1.038590701(22)	-77727.9(26)	-77725(123)	[23]
	$^{136}\text{Te}$	1.046316045(24)	-74425.7(29)	-74430(50)	[18]
	$^{137}\text{Te}$	1.054056424(21)	-69304.2(25)	-69290(120)	[23]
	$^{138}\text{Te}$	1.061784295(36)	-65696(5)	-65755(122)	[23]
	$^{139}\text{Te}$	1.069527729(29)	-60205(4)		
	$^{140}\text{Te}$	1.07725759(23)	-56357(27)		

<sup>x</sup> corrected for 65.1 keV isomer, see Ref. [18]

<sup>†</sup> isomer separated

Two-neutron separation energies ( $S_{2n}$ ) across the  $N=82$  neutron number including Penning trap data from the present work and those from Refs. [7, 8, 19–22, 24, 25] are shown in Fig. 3 for even neutron isotones from  $N=78$  to 88. A smooth dependence of  $S_{2n}$  on the proton number, and the sharp drop from  $N=82$  to  $N=84$ , high-

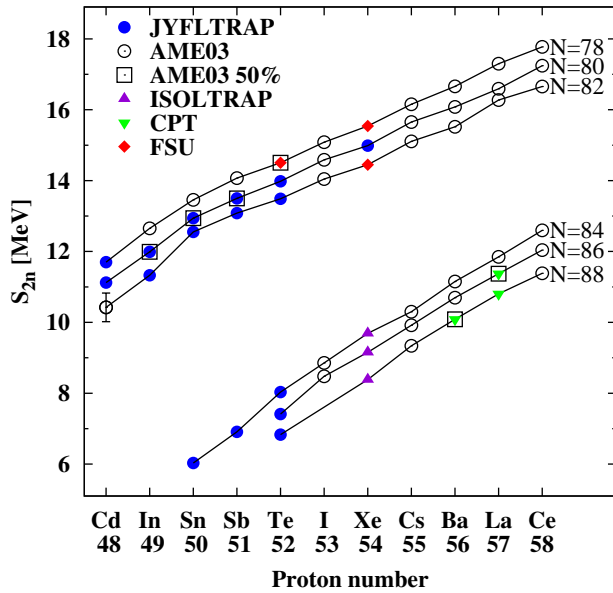


FIG. 3. (Color online) Experimental two-neutron separation energies as a function of proton number for  $N=78-88$  isotones. For the squared points one of the masses is taken from AME03.

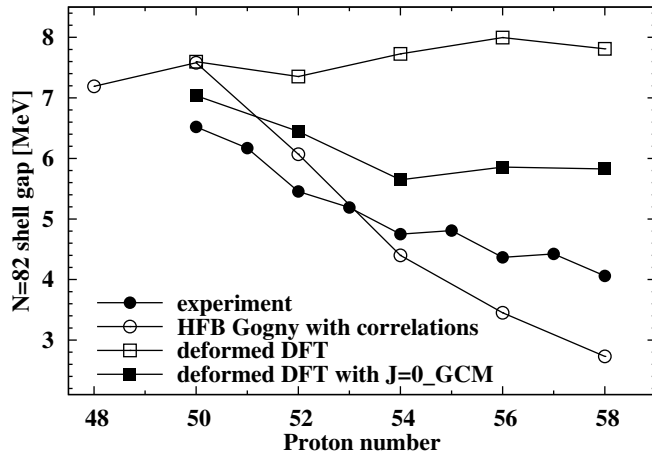


FIG. 4.  $N=82$  shell gap energy as a function of proton number. See text for details.

light a large shell gap. The evolution of the shell gap  $\Delta = S_{2n}(N=82) - S_{2n}(N=84)$  as a function of the proton number, shown in Fig. 4, demonstrates the strength of the gap even more clearly. The  $N=82$  gap is rather slowly decreasing towards larger  $Z$  values. In order to learn about the possible role of correlations in the shell-gap energy, Fig. 4 also shows values calculated with three mean-field approaches. The calculation of Bender *et al.* [26] employing the SLy4 [27] energy density functional in the deformed basis with dynamical quadrupole correlations (deformed DFT with  $J=0\_GCM$ ) shows reasonably good agreement with experimental data although it is not able to explain the reduction sufficiently, unlike in the case

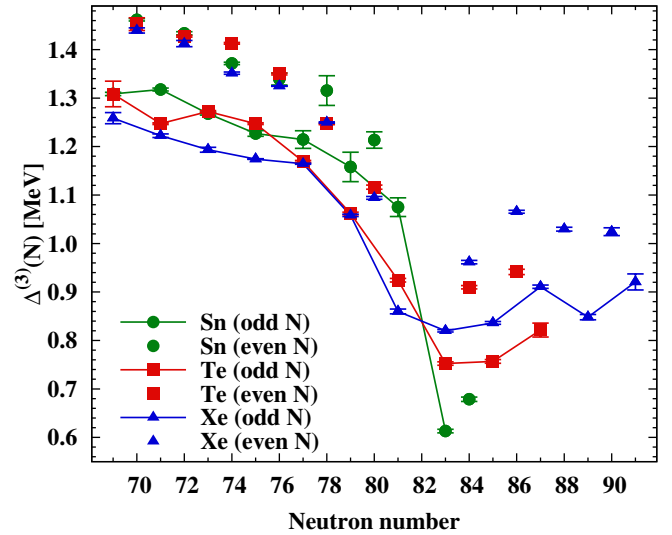


FIG. 5. (Color online) Experimental odd-even mass staggering for Sn, Te, and Xe isotope chains. The data points for  $N=82$  are beyond the scale.

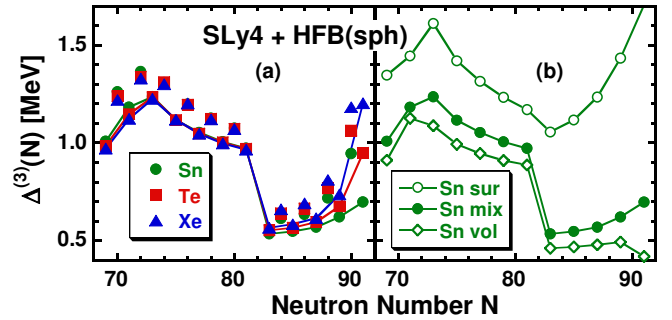


FIG. 6. (Color online) Calculated (spherical HFB) odd-even mass staggering for Sn, Te, and Xe isotope chains. For clarity, the odd- $N$  points have been connected with lines.

of  $N=50$  [28]. The same calculation without correlations gives results rather insensitive to the proton number, which suggests that the dependence of the shell gap can be here attributed to a weak influence of core-polarisation effects. Another interesting comparison is provided by the recent approach of Goriely *et al.* [29] employing the HFB framework with a Gogny interaction and taking into account all the quadrupole correlations self-consistently and microscopically (HFB Gogny with correlations). This model provides too strong reduction for the gap energy with increasing  $Z$  but reproduces the gap near  $Z=50$  equally well with the other two calculations. In conclusion, it is obvious that the mean-field models such as those in Refs. [26, 29] rather successfully describe the binding energies near the shell closures. At  $Z=50$  and  $N=82$  the over-prediction of the gap is only about 0.5 MeV.

The high precision of Penning-trap mass measurements opens a possibility to study the odd-even staggering of binding energies and related empirical pairing gaps of ex-

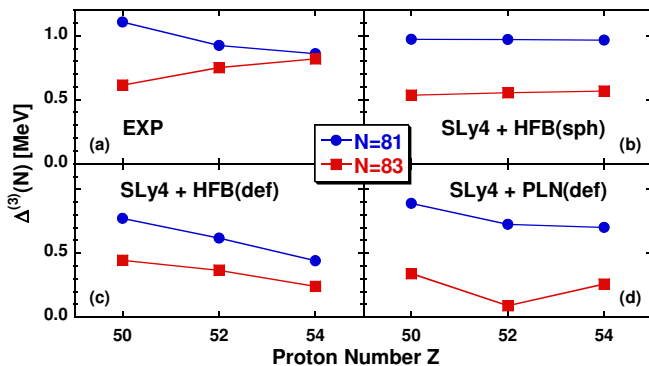


FIG. 7. (Color online) Odd-even staggering for the  $N=81$  and  $83$  isotones.

otic weakly bound nuclei. The most simple example is the three-point odd-even-mass-staggering formula [6]

$$\Delta^{(3)}(N) = (-1)^N [E(N+1) - 2E(N) + E(N-1)]/2, \quad (2)$$

where  $N$  is the number of nucleons (neutrons or protons) and  $E$  the binding energy. Figure 5 shows the experimental neutron  $\Delta^{(3)}$  staggering for Sn, Te, and Xe isotopes crossing the  $N=82$  shell closure. The other 3-point indicator corresponding to the even neutron numbers is less interesting for this purpose because it is more sensitive to the splitting of the single-particle spectrum around the Fermi level [6, 30]. The difference between the values at  $N=81$  and  $83$  shows a large asymmetry for Sn but a much smaller one for Te and Xe. This indicates a considerably stronger quenching in pairing gap for Sn than for Te and Xe suggesting the importance of core polarisation effects. This is somewhat discrepant to the behaviour of the shell gap energy shown in Fig. 4. A similar asymmetry observed for  $B(E2)$  values of n-rich Te isotopes was also traced to reduced neutron pairing above the  $N=82$  shell closure [4].

In order to probe this question theoretically, we performed self-consistent calculations of varying complexity, by using the Sly4 [27] energy density functional and contact pairing force. To make a meaningful comparison, in each variant of the calculation, the pairing strength (equal for neutrons and protons) was adjusted so as to give the average pairing gap in  $^{120}\text{Sn}$  equal to 1.245 MeV. The pairing channel was described within the HFB approximation and the blocking and filling approximations [30, 31] were used to treat odd nuclei.

First, to provide a baseline for further analyses, in Fig. 6 we show the neutron  $\Delta^{(3)}$  staggering calculated within the spherical approximation [32]. From Fig. 6b we see that for the volume (vol) or mixed (mix) pairing forces [33], the experimental decrease of  $\Delta^{(3)}$  when crossing the  $N=82$  gap in Sn is very well reproduced, whereas the data exclude the pure surface pairing force. Such pairing decrease is due to a lower level density above the  $N=82$  gap [4] (the surface pairing force is unable to discriminate between the two surface-type orbitals  $\nu h_{11/2}$  and  $\nu f_{7/2}$  located below

and above the  $N=82$  shell gap, respectively). Spherical calculations miss the experimental values in Te and Xe isotopes (Fig. 6a).

To better illustrate the trends in  $Z > 50$  nuclei, in Fig. 7 we show the experimental neutron  $\Delta^{(3)}$  staggering in Sn, Te, and Xe isotopes along the  $N=81$  and  $83$  lines, compared with theoretical results. In experiment (Fig. 7a), the difference between the  $N=81$  and  $83$  isotones smoothly decreases from about 0.5 MeV in Sn to almost zero in Xe, whereas spherical results (Fig. 7b) show no such a decrease at all. To analyse the effects of correlations induced by deformation effects, we show in Fig. 7c the analogous results obtained within the deformed HFB calculations by using the code HFODD (v2.51i) [34], and in Fig. 7d those obtained within the Lipkin-Nogami method followed by the exact particle-number projection (PLN), and by using the HFBTHO code [35, 36].

In the deformed HFB calculations, the even isotones,  $N=80, 82,$  and  $84,$  turn out to be spherical whereas the odd-particle polarisation induces a non-zero deformation in the odd isotones,  $N=81$  and  $83.$  Therefore, the odd-particle polarisation induces lower values of the  $\Delta^{(3)}$  staggering solely through the lowering of energies of odd isotones. Since such polarisation increases with adding protons, values of  $\Delta^{(3)}$  decrease with  $Z,$  and this effect is identical on both sides of the  $N=82$  shell gap (Fig. 7c), at variance with experiment. This picture is not qualitatively changed by using the particle-number conserving approach (Fig. 7d), in which the pairing correlations, becoming non-zero in the  $N=82$  isotones, lead to larger values of the  $\Delta^{(3)}$  staggering, and in the  $N=81$  isotones perfectly well reproduce the experimental trend. However, in the  $N=83$  isotones, the disagreement with data remains a puzzle, unresolved within the current state of the art theoretical approaches.

In conclusion, precise mass measurements in exotic nuclei allow us to look into the fine structure effects of these systems, to challenge standard theoretical approaches, and thus to call for the development of new methods. The data clearly exclude the pure surface-localised pairing forces. In addition, the  $Z$  dependence of the neutron odd-even mass staggering in the  $N=83$  isotones cannot be explained by the combined pairing and static-deformation correlation effects. Study of higher-order correlations, such as the configuration mixing of deformed states, requires an implementation of methods for odd nuclei that are presently not available.

This work has been supported by the Academy of Finland under the Centre of Excellence Programme 2006–2014 (Nuclear and Accelerator Based Physics Programme at JYFL) and the FIDIPRO program.

\* jani.hakala@phys.jyu.fi

- † *Present address:* Max-Planck-Institut für Kernphysik, Saupfercheckweg 1, 69117 Heidelberg, Germany
- ‡ juha.aysto@phys.jyu.fi
- [1] P. Hoff *et al.* (ISOLDE Collaboration), *Phys. Rev. Lett.* **77**, 1020 (Aug 1996)
- [2] K. L. Jones, A. S. Adekola, D. W. Bardayan, J. C. Blackmon, K. Y. Chae, K. A. Chipps, J. A. Cizewski, L. Erikson, C. Harlin, R. Hatarik, R. Kapler, R. L. Kozub, J. F. Liang, R. Livesay, Z. Ma, B. H. Moazen, C. D. Nesaraja, F. M. Nunes, S. D. Pain, N. P. Patterson, D. Shapira, J. F. Shriner, M. S. Smith, T. P. Swan, and J. S. Thomas, *Nature* **465**, 454 (May 2010)
- [3] D. C. Radford, C. Baktash, J. R. Beene, B. Fuentes, A. Galindo-Uribarri, C. J. Gross, P. A. Hausladen, T. A. Lewis, P. E. Mueller, E. Padilla, D. Shapira, D. W. Stracener, C.-H. Yu, C. J. Barton, M. A. Caprio, L. Coraggio, A. Covello, A. Gargano, D. J. Hartley, and N. V. Zamfir, *Phys. Rev. Lett.* **88**, 222501 (May 2002)
- [4] J. Terasaki, J. Engel, W. Nazarewicz, and M. Stoitsov, *Phys. Rev. C* **66**, 054313 (Nov 2002)
- [5] M. P. Kartamyshev, T. Engeland, M. Hjorth-Jensen, and E. Osnes, *Phys. Rev. C* **76**, 024313 (Aug 2007)
- [6] W. Satuła, J. Dobaczewski, and W. Nazarewicz, *Phys. Rev. Lett.* **81**, 3599 (Oct 1998)
- [7] M. Dworschak, G. Audi, K. Blaum, P. Delahaye, S. George, U. Hager, F. Herfurth, A. Herlert, A. Kellerbauer, H.-J. Kluge, D. Lunney, L. Schweikhard, and C. Yazidjian, *Phys. Rev. Lett.* **100**, 072501 (Feb 2008)
- [8] D. Neidherr, R. B. Cakirli, G. Audi, D. Beck, K. Blaum, C. Böhm, M. Breitenfeldt, R. F. Casten, S. George, F. Herfurth, A. Herlert, A. Kellerbauer, M. Kowalska, D. Lunney, E. Minaya-Ramirez, S. Naimi, M. Rosenbusch, S. Schwarz, and L. Schweikhard, *Phys. Rev. C* **80**, 044323 (Oct 2009)
- [9] M. Arnould, S. Goriely, and K. Takahashi, *Physics Reports* **450**, 97 (2007)
- [10] A. Jokinen, T. Eronen, U. Hager, I. Moore, H. Penttilä, S. Rinta-Antila, and J. Äystö, *Int. J. Mass Spectrom.* **251**, 204 (Apr. 2006)
- [11] H. Penttilä, J. Billowes, P. Campbell, P. Dendooven, V. Elomaa, T. Eronen, U. Hager, J. Hakala, J. Huikari, A. Jokinen, A. Kankainen, P. Karvonen, S. Kopecky, B. Marsh, I. Moore, A. Nieminen, A. Popov, S. Rinta-Antila, Y. Wang, and J. Äystö, *Eur. Phys. J. A* **25**, 745 (Sep. 2005)
- [12] G. Savard, S. Becker, G. Bollen, H. J. Kluge, R. B. Moore, T. Otto, L. Schweikhard, H. Stolzenberg, and U. Wiess, *Phys. Lett. A* **158**, 247 (Sep. 1991)
- [13] T. Eronen, V.-V. Elomaa, U. Hager, J. Hakala, A. Jokinen, A. Kankainen, S. Rahaman, J. Rissanen, C. Weber, and J. Äystö, *Nucl. Instrum. Methods Phys. Res., Sect. B* **266**, 4527 (Oct. 2008)
- [14] M. König, G. Bollen, H.-J. Kluge, T. Otto, and J. Szerypo, *Int. J. Mass Spectrom. Ion Processes* **142**, 95 (1995)
- [15] S. George, K. Blaum, F. Herfurth, A. Herlert, M. Kretschmar, S. Nagy, S. Schwarz, L. Schweikhard, and C. Yazidjian, *Int. J. Mass Spectrom.* **264**, 110 (2007)
- [16] J. Hakala, R. Rodríguez-Guzmán, V. Elomaa, T. Eronen, A. Jokinen, V. Kolhinen, I. Moore, H. Penttilä, M. Reponen, J. Rissanen, A. Saastamoinen, and J. Äystö, *Eur. Phys. J. A* **47**, 1 (2011)
- [17] T. Eronen, V.-V. Elomaa, J. Hakala, J. C. Hardy, A. Jokinen, I. D. Moore, M. Reponen, J. Rissanen, A. Saastamoinen, C. Weber, and J. Aysto, *Phys. Rev. Lett.* **103**, 252501 (Dec. 2009)
- [18] G. Audi, A. H. Wapstra, and C. Thibault, *Nucl. Phys. A* **729**, 337 (2003)
- [19] M. Redshaw, B. J. Mount, E. G. Myers, and F. T. Avignone, *Phys. Rev. Lett.* **102**, 212502 (May 2009)
- [20] M. Redshaw, B. J. Mount, and E. G. Myers, *Phys. Rev. A* **79**, 012506 (Jan 2009)
- [21] G. Sikler, G. Audi, D. Beck, K. Blaum, G. Bollen, F. Herfurth, A. Kellerbauer, H.-J. Kluge, D. Lunney, M. Oinonen, C. Scheidenberger, S. Schwarz, and J. Szerypo, *Nucl. Phys. A* **763**, 45 (Dec. 2005)
- [22] M. Breitenfeldt *et al.*, *Phys. Rev. C* **81**, 034313 (Mar. 2010)
- [23] B. Sun *et al.*, *Nucl. Phys. A* **812**, 1 (2008)
- [24] M. Redshaw, E. Wingfield, J. McDaniel, and E. G. Myers, *Phys. Rev. Lett.* **98**, 053003 (Feb 2007)
- [25] G. Savard, J. Wang, K. Sharma, H. Sharma, J. Clark, C. Boudreau, F. Buchinger, J. Crawford, J. Greene, S. Gulick, A. Hecht, J. Lee, A. Levand, N. Scielzo, W. Trimble, J. Vaz, and B. Zabransky, *Int. J. Mass Spectrom.* **251**, 252 (2006)
- [26] M. Bender, G. F. Bertsch, and P.-H. Heenen, *Phys. Rev. C* **78**, 054312 (Nov 2008)
- [27] E. Chabanat, P. Bonche, P. Haensel, J. Meyer, and R. Schaeffer, *Nucl. Phys. A* **635**, 231 (1998)
- [28] J. Hakala, S. Rahaman, V.-V. Elomaa, T. Eronen, U. Hager, A. Jokinen, A. Kankainen, I. D. Moore, H. Penttilä, S. Rinta-Antila, J. Rissanen, A. Saastamoinen, T. Sonoda, C. Weber, and J. Äystö, *Phys. Rev. Lett.* **101**, 052502 (2008)
- [29] S. Goriely, S. Hilaire, M. Girod, and S. Péru, *Phys. Rev. Lett.* **102**, 242501 (Jun 2009)
- [30] G. Bertsch, J. Dobaczewski, W. Nazarewicz, and J. Pei, *Phys. Rev. A* **79**, 043602 (Apr 2009)
- [31] N. Schunck, J. Dobaczewski, J. McDonnell, J. Moré, W. Nazarewicz, J. Sarich, and M. V. Stoitsov, *Phys. Rev. C* **81**, 024316 (Feb 2010)
- [32] J. Dobaczewski, H. Flocard, and J. Treiner, *Nucl. Phys. A* **422**, 103 (1984)
- [33] J. Dobaczewski, W. Nazarewicz, and M. Stoitsov, *Eur. Phys. J. A* **15**, 21 (2002)
- [34] N. Schunck, J. Dobaczewski, J. McDonnell, W. Satuła, J. Sheikh, A. Staszczak, M. Stoitsov, and P. Toivanen, *Comp. Phys. Commun.* **183**, 166 (2012)
- [35] M. Stoitsov, J. Dobaczewski, W. Nazarewicz, and P. Ring, *Comp. Phys. Commun.* **167**, 43 (2005)
- [36] M. V. Stoitsov, J. Dobaczewski, R. Kirchner, W. Nazarewicz, and J. Terasaki, *Phys. Rev. C* **76**, 014308 (Jul 2007)